

ChemPhysChem

Supporting Information

The Elusive Ketene (H_2CCO) Channel in the Infrared Multiphoton Dissociation of Solid 1,3,5-Trinitro-1,3,5-Triazinane (RDX)

Santosh K. Singh, Jesse La Jeunesse, Vasant Vuppuluri, Steven F. Son, Bing-Jian Sun, Yue-Lin Chen, Agnes H. H. Chang, Alexander M. Mebel, and Ralf I. Kaiser*

Experimental Methods

The experiments were conducted in an ultrahigh vacuum (UHV) chamber evacuated to a base pressure of 2×10^{-10} torr utilizing magnetically levitated turbo molecular pumps coupled to oil-free dry scroll pumps.^[1] A polished silver substrate is coated with a film of RDX at a thickness of $15.5 \pm 1.0 \mu\text{m}$ via the drop-casting method (sample preparation). This substrate is sandwiched with indium foil to an oxygen-free high conductivity copper (OFHC) cold finger, which in turn is connected to a closed cycle helium refrigerator (Sumitomo Heavy Industries, RDK-415E). This unit can cool the substrate to temperatures as low as $5.0 \pm 0.1 \text{ K}$. A silicon diode sensor (Lakeshore DT-670) and a cartridge heater are attached to the cold finger to monitor and control the temperature of the substrate. This entire assembly is freely rotatable horizontally exploiting a doubly differentially pumped rotary feedthrough (Thermoionics Vacuum Products, RNN-600/FA/MCO) and translatable vertically with the help of a UHV compatible bellow (McAllister, BLT106). A Fourier-transform infrared spectrometer (FTIR; Nicolet 6700) was employed to record the infrared (IR) spectra of the RDX samples at 5 K covering the region $4000\text{-}500 \text{ cm}^{-1}$ and at a resolution of 4 cm^{-1} (Figure S1-S2, Table S1). All FTIR measurements were performed in absorption-reflection-absorption mode at a reflection angle of 45° to the substrate normal. The thickness of RDX film was determined using equation (1)

$$d = \frac{N}{2\sqrt{n^2 - \sin^2 \theta} (v_1 - v_2)} \quad (1)$$

where d is the thickness of the film, N is the number of interference fringes observed in the FTIR spectrum due to fringing effect, n is the refractive index of RDX ($n = 1.49$)⁴, θ is the angle of incidence (45°), v_1 and v_2 are the start and end points of the spectrum in cm^{-1} covering the fringes. After acquiring the reference IR spectrum of the RDX samples, each film was exposed to pulsed carbon dioxide (CO_2) IR laser (SYNRAD Firestar v40; $10.6 \mu\text{m}$) at an angle of 0° relative to the normal of the substrate. The CO_2 laser used in this study has a pulse width of $200 \mu\text{s}$ and operates at a repetition rate of 5 kHz . The laser beam shape was circular with a radius of $0.50 \pm 0.05 \text{ cm}$. The samples were exposed to average laser power of 10 W (low dose) as well as 24 W (high dose) for 4 hours over an area of $0.8 \pm 0.1 \text{ cm}^2$. The total energy deposited at low dose and high dose is $1.80 \pm 0.2 \times 10^5 \text{ J cm}^{-2}$ and $4.32 \pm 0.5 \times 10^5 \text{ J cm}^{-2}$ respectively. The penetration depth of the laser is calculated to be $3.6 \pm 0.3 \mu\text{m}$ via equation 2

$$\delta = \frac{\lambda}{4\pi\kappa} \quad (2)$$

where δ is the penetration depth, λ is the wavelength of the IR laser ($10.6 \mu\text{m}$) and κ is the imaginary part of the complex refractive index. For RDX the value of κ at $10.6 \mu\text{m}$ was determined to 0.236 .^[2]

To calculate the irradiation dose at high laser power (24 W for 4 hours), the following equations were used:

$$\text{Energy per pulse (J)} = \frac{\text{Average power (W)}}{\text{Repetition rate (Hz)}} = \frac{24 \text{ W}}{5000 \text{ Hz}} = 0.0048 \text{ J} = 4.8 \text{ mJ} \quad (3)$$

$$\text{Total number of pulse} = \text{Repetition rate (s}^{-1}\text{)} \times \text{total irradiation time (s)} \quad (4)$$

$$= 5000 \text{ s}^{-1} \times 14400 \text{ s} = 7.2 \times 10^7$$

$$\begin{aligned} \text{Total deposited energy per unit area (J cm}^{-2}\text{)} &= \frac{\text{Energy per pulse (J)} \times \text{Total number of pulse}}{\text{Area of the beam spot (cm}^2\text{)}} \quad (5) \\ &= \frac{0.0048 \text{ J} \times 7.2 \times 10^7}{0.8 \pm 0.1 \text{ cm}^2} = 4.32 \pm 0.5 \times 10^5 \text{ J cm}^{-2} \end{aligned}$$

$$\begin{aligned} \text{Dose in eV molecule}^{-1} &= \frac{\text{Total deposited energy per unit area (J cm}^{-2}\text{)} \times 6.24 \times 10^{18}}{\text{Column density calculated for IR band at } 1581 \text{ cm}^{-1} (\text{molecules cm}^{-2})} \quad (6) \\ &= \frac{4.32 \pm 0.5 \times 10^5 \text{ J cm}^{-2}}{2.0 \pm 0.2 \times 10^{18} \text{ molecules cm}^{-2}} \times (6.24 \times 10^{18}) \\ &= 1.35 \pm 0.2 \times 10^6 \text{ eV molecule}^{-1} \end{aligned}$$

After the irradiation, the exposed samples were annealed from 5 K to 320 K at a rate of 1 K min^{-1} (temperature programmed desorption; TPD). During the TPD phase, the molecules subliming from the substrate were monitored using photoionization reflectron time-of-flight mass spectrometer (PI-ReTOF-MS). In the PI-ReTOF-MS setup, we exploit pulsed vacuum ultraviolet (VUV) light at 10.49 eV and 9.30 eV to softly photoionize the subliming molecules. By tuning the photoionization energy from 10.49 eV to 9.30 eV , we determined which structural isomer(s), diazomethane (H_2CNN) and/or ketene (H_2CCO) are/is detected at mass-to-charge (m/z) of 42 in the processed RDX. The ions produced in the photoionization process of the neutrals are then separated in the reflectron time-of-flight tube based on their mass-to-charge ratio and eventually

detected via a dual chevron configured microchannel plate (MCP) detector (Jordan TOF Products Inc.). The MCP detector generates the signal which is amplified via a pre-amplifier (Ortec 9305) and shaped with a 100 MHz discriminator (Advanced Research Instruments Corporation; F-100TD). A computer-based multichannel scaler receives the signal from the discriminator and records it using 4 ns bin widths triggered at 30 Hz by a pulse delay generator (Quantum Composers 9518). 3600 sweeps are collected per mass spectrum per 1 K increase in the temperature during the TPD phase.

Computational methods

The reactions of (1) RDX decomposition to three H₂CNNO₂ molecules, (2) H₂CNNO₂ dissociation to formaldehyde (H₂CO) and dinitrogen monoxide (N₂O), and (3) formation of ketene (H₂CCO) plus water via two formaldehyde molecules are investigated on adiabatic singlet ground-state potential energy surfaces, respectively. Likely reaction channels are identified such that intermediates and transition states are located. With B3LYP/cc-pVTZ^[3] calculations, their geometries are optimized and corresponding harmonic frequencies computed. Subsequently, the CCSD(T)/cc-pVDZ, CCSD(T)/cc-pVTZ, and CCSD(T)/cc-pVQZ energies^[4] are also obtained and then extrapolated to complete basis set limits,^[5] CCSD(T)/CBS, with B3LYP/cc-pVTZ zero-point energy corrections. The potential energy surface for the decomposition of RDX into diazomethane (H₂CNN) is also calculated at the same level of theory for comparison. The energies are accurate within 8 kJ mol⁻¹. All the calculations were performed using Gaussian 16 program package.^[6]

Sample Preparation

RDX samples were received from BAE Systems, Inc. prepared according to the MIL-DTL-398 D (Military Specification, Detail Specification RDX, 12 DEC 1996); this specifies an HMX (1,3,5,7-tetranitro-1,3,5,7-tetrazoctane; C₄H₈N₈O₈) impurity in RDX at levels from 4 % to 17 %. The maximum permissible quantity of other impurities if present is 0.08 %. In order to remove the impurities, production grade RDX was recrystallized from acetone (Fisher Scientific, Inc.). Nuclear magnetic resonance (NMR) spectroscopy was exploited to characterize the recrystallized RDX. Figure S9 of the supporting information shows the ¹³C NMR spectra of the crude and recrystallized RDX measured using a Spinsolve 60 Carbon benchtop 60 MHz NMR spectrometer

after dissolving in dimethylsulfoxide-d6 (DMSO-d6) solvent. The disappearance of the peaks associated with the chemical shift of HMX indicates that RDX has been sufficiently purified to a level of at least 99.9 %.^[7] A thin film of RDX onto the silver substrate was prepared using a drop-casting method. For the drop-casting, about 2 mg of recrystallized (purified) RDX is dissolved in 3 g of methyl ethyl ketone (MEK; Acros Organics) inside a vial. Sonication and mild heating at 305 K ensure complete dissolution of the RDX in MEK. Using a glass pipette, a drop of RDX/MEK solution was deposited onto the silver substrate and then left for drying. A uniform layer of RDX is observed after the evaporation of solvent and characterized via infrared spectroscopy.

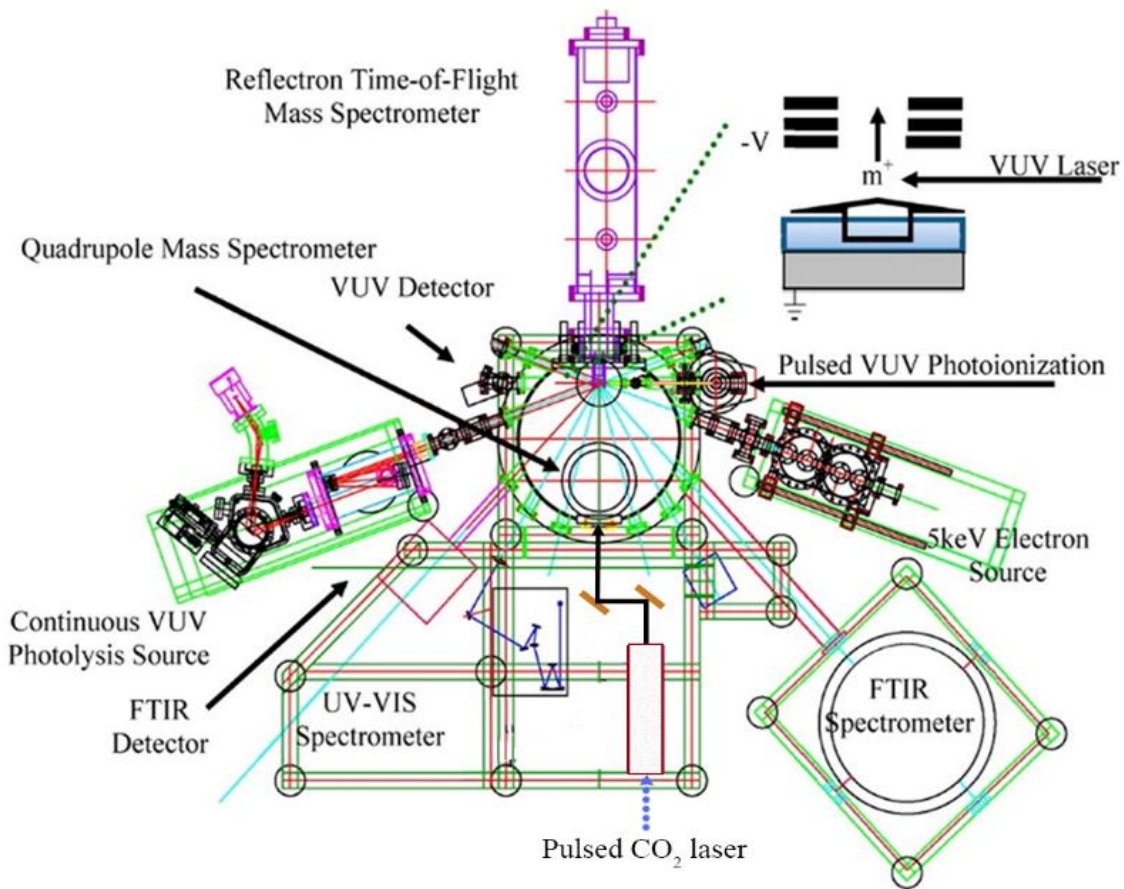


Figure S1. Schematic top view of the ultra-high vacuum chamber including the radiation sources (electron source, pulsed CO₂ laser), analytical instruments (FTIR, UV-VIS, ReTOF), and cryogenic target (point of convergence lines).^[1]

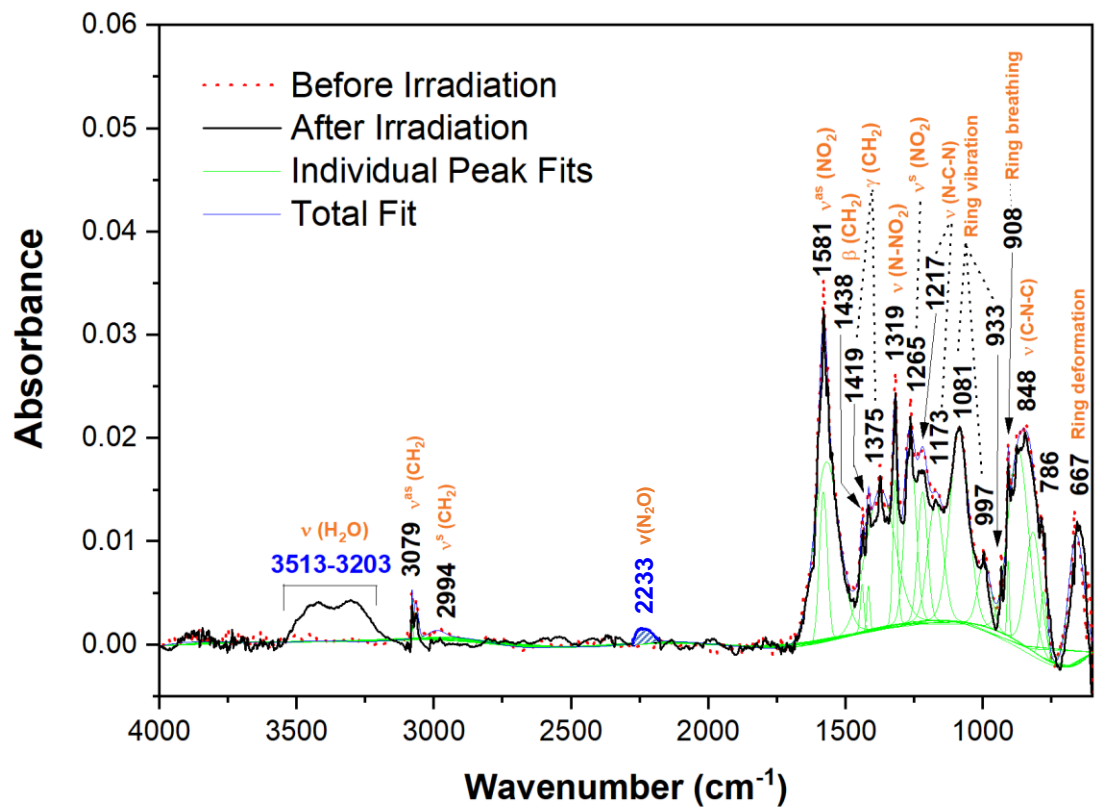


Figure S2. Infrared (IR) spectra of RDX collected at 5 K before the irradiation (red-dotted) and after the irradiation at high dose (black-solid). Deconvolution of IR spectrum measured after the irradiation is not presented here for better clarity. The shaded peak at 2233 cm^{-1} is predicted for N=N stretch of N_2O based on its integrated absorption coefficient and observed column density of H_2O (for details see quantitative analysis). Based on the calculated peak curve for N_2O it can be argued that the IR band corresponding to N_2O is within the noise of the IR background therefore, it is difficult to observe/assign in the spectrum measured after the irradiation.

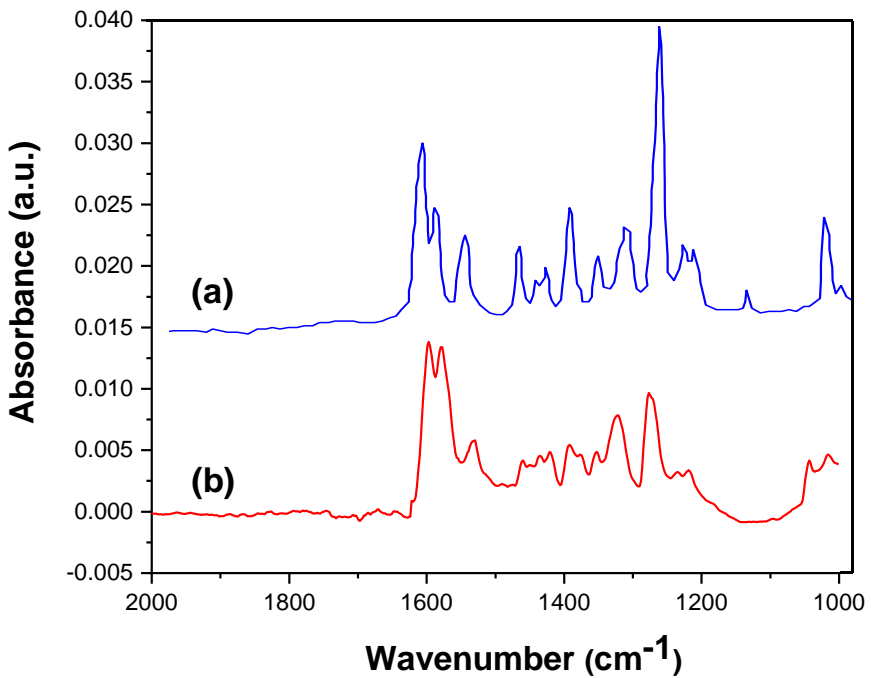


Figure S3. Infrared spectra of (a) crystalline phase of RDX film measured by Botcher, T. R. *et al.* (b) amorphous phase of RDX film measured in this study. Fig (a) is adapted with permission from Botcher, T. R.; Wight, C. A. *J. Phys. Chem.* **1993**, *97*, 9149-9153. Copyright (1993) American Chemical Society.

IR quantitative analysis: Mass balance

The column densities were calculated using a modified Lambert-Beer law to determine the amount of RDX molecules destroyed and that of products formed.^[8] The integrated absorption co-efficient of the reactant (RDX) and products (H_2O , N_2O) used for the calculation of column densities are taken from literature. The absorption coefficient of RDX band at 1581 cm^{-1} is $1.0 \times 10^{-18} \text{ cm molecule}^{-1}$. The column density of H_2O (water) is measured in the region of $3513\text{-}3203 \text{ cm}^{-1}$ using an integrated band strength of $2.0 \times 10^{-16} \text{ cm molecule}^{-1}$.^[9] The column density of N_2O (dinitrogen monoxide) is calculated based on the integrated absorption coefficient of N=N stretch of N_2O (2233 cm^{-1}) i.e. $5.7 \times 10^{-17} \text{ cm molecule}^{-1}$ and observed column density of H_2O (water).^[10] The amount of RDX molecules destroyed via the irradiation is $1.4 \pm 0.2 \times 10^{15} \text{ molecules cm}^{-2}$, i.e. 8 % of the initial column density ($1.8 \pm 0.3 \times 10^{16} \text{ molecules cm}^{-2}$). The total number of H_2O molecules formed is $0.40 \pm 0.04 \times 10^{15} \text{ molecules cm}^{-2}$. Based on the observed column density of H_2O (water) we calculated the possible number of N_2O molecules formed, which is equal to $0.80 \pm 0.08 \times 10^{15} \text{ molecules cm}^{-2}$. The predicted peak curve for N=N stretch of N_2O is shown in Figure S2. The amount of H_2O molecules formed and predicted amount of N_2O could account for 87 ± 15 % of decomposed RDX molecules.

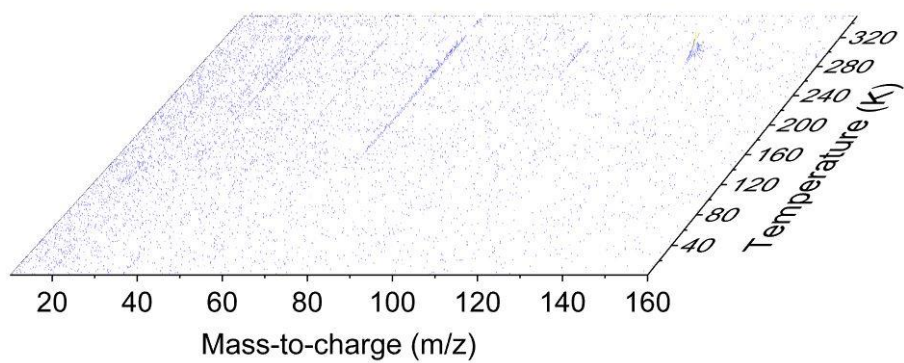


Figure S4. PI-ReTOF mass spectrum measured as a function of temperature in a blank experiment at a photoionisation energy of 10.49 eV.

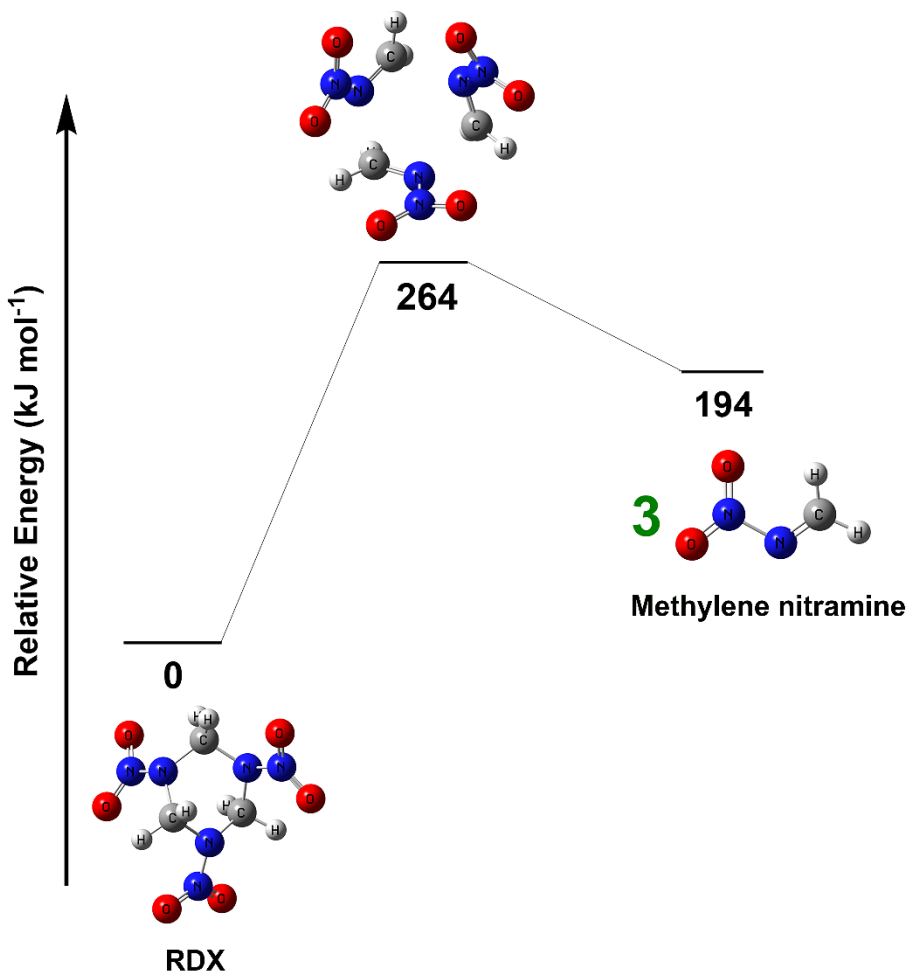
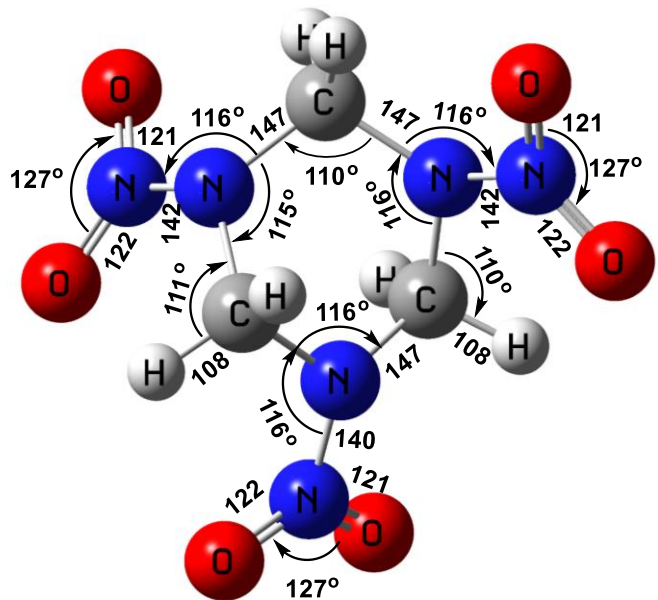
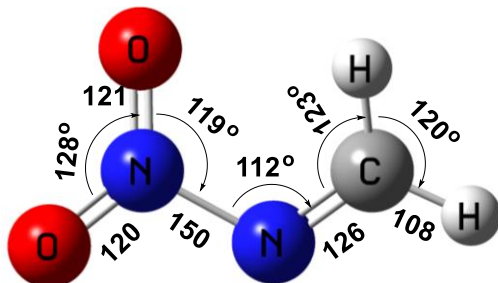


Figure S5. Theoretically predicted reaction pathway of unimolecular decomposition of RDX via triple concerted C-N bond scission leading to methylene nitramine (H_2CNNO_2).



1,3,5-Trinitro-1,3,5-triazinane (RDX; C₃H₆N₆O₆)



Methylene nitramine (H_2CNNO_2)

Figure S6. Structures and geometrical parameters of RDX (reactant) and methylene nitramine (product) calculated at the B3LYP/cc-pVTZ//CCSD(T)/CBS level of theory. Bond lengths are in pm and bond angles are in degrees.

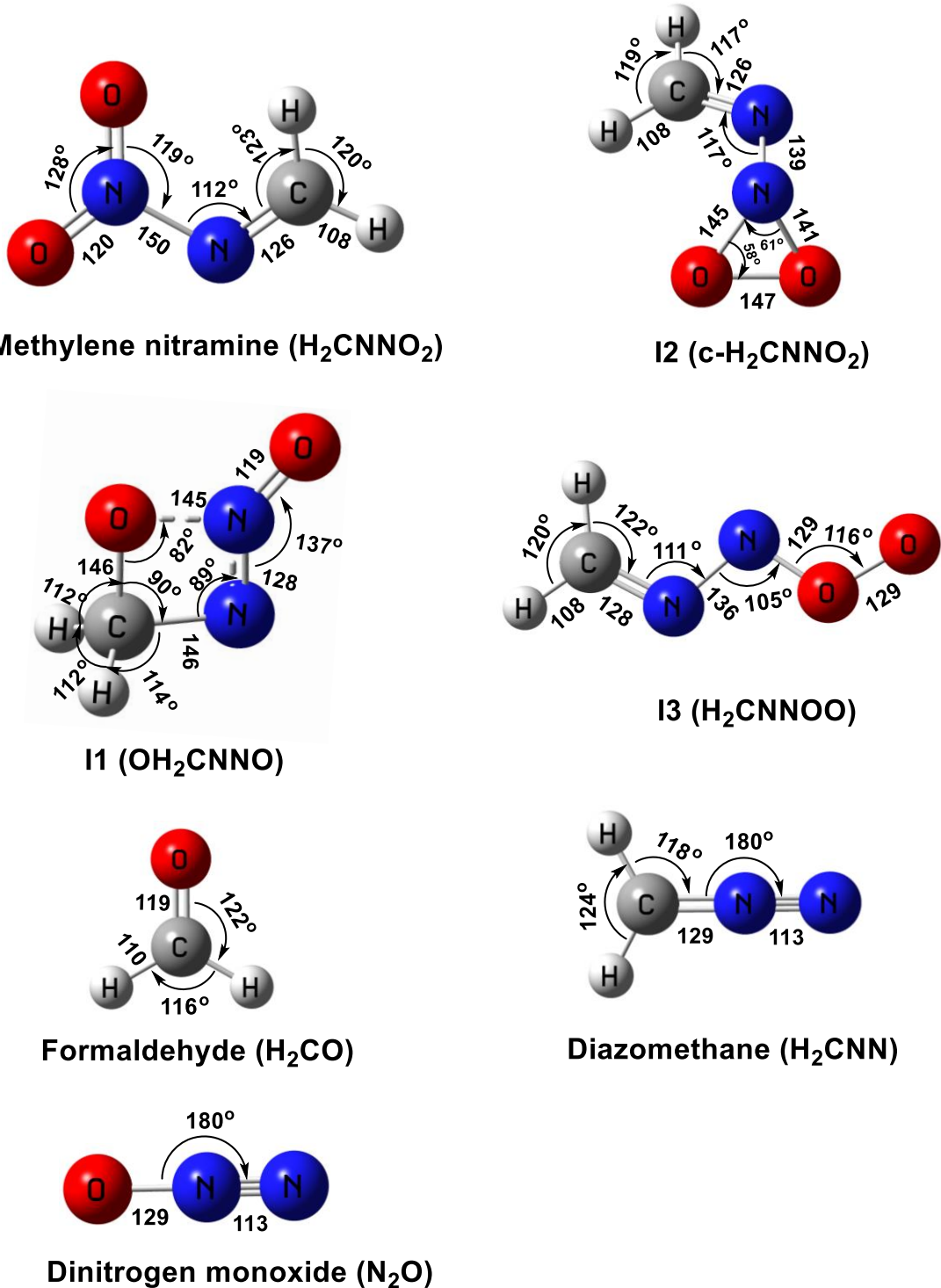
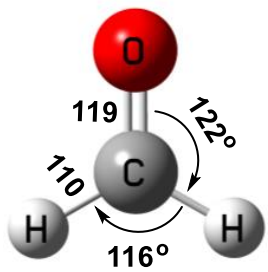
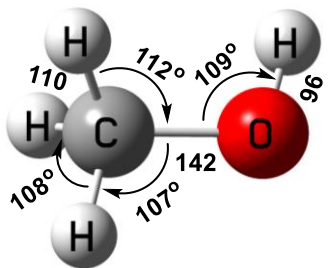


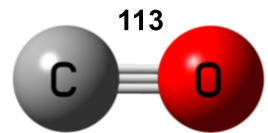
Figure S7. Calculated structures and geometrical parameters of reactant (methylene nitramine), intermediates (I1, I2 and I3) and products (formaldehyde, diazomethane and dinitrogen monoxide). Bond lengths are in pm and bond angles are in degrees.



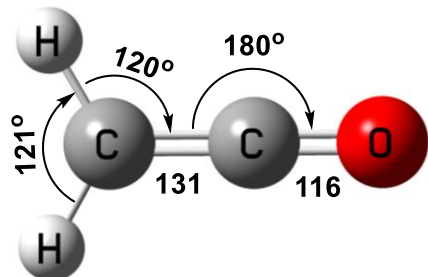
Formaldehyde (H_2CO)



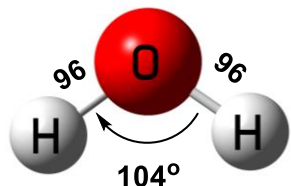
Methanol (CH_3OH)



Carbon monoxide (CO)



Ketene (H_2CCO)



Water (H_2O)

Figure S8. Calculated structures and geometrical parameters of reactant (formaldehyde), intermediates (methanol, carbon monoxide) and products (ketene, water). Bond lengths are in pm and bond angles are in degrees.

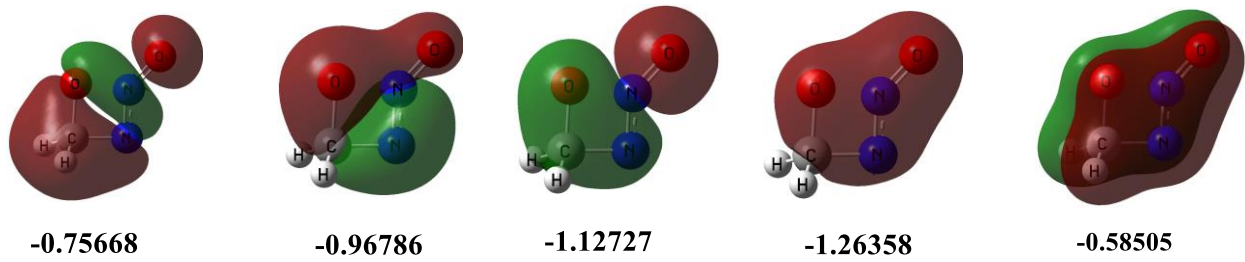


Figure S9. Molecular orbital diagram of intermediate I1 (c-OH₂CNNO) depicting electron density on the heteroatoms and over the ring.

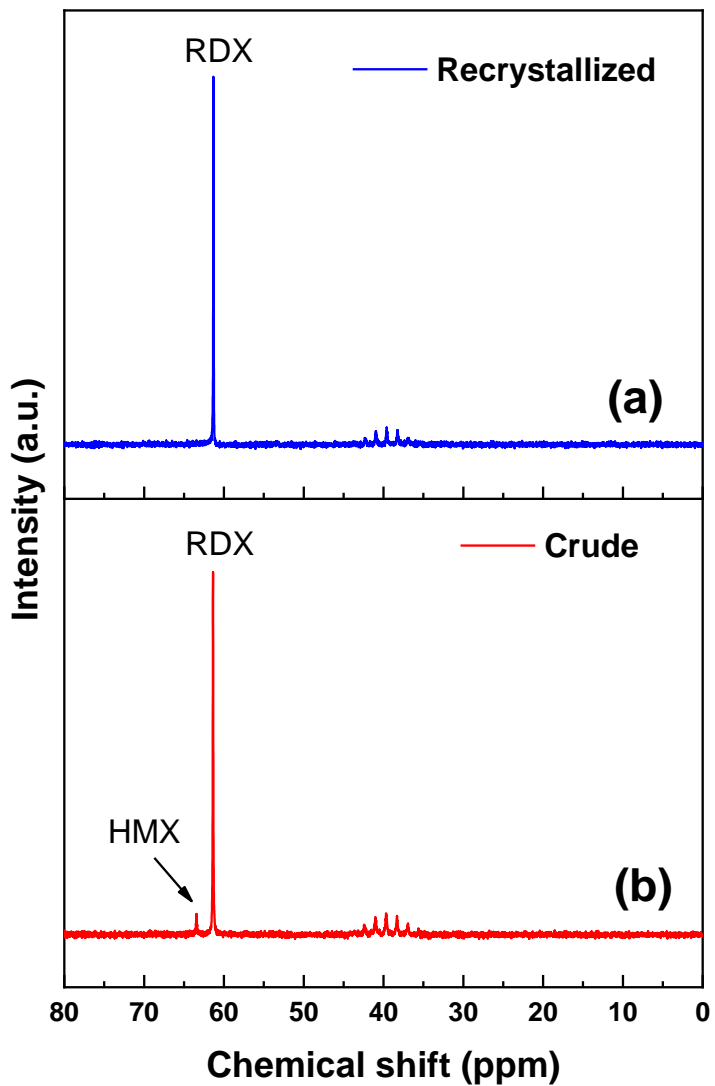


Figure S10. ^{13}C NMR spectra of (a) recrystallized RDX (b) crude RDX. Peak at 63.47 ppm in the NMR spectra of crude RDX corresponds to HMX impurity which is absent in the NMR spectra measured after recrystallization of RDX.

Table S1. (a) Infrared features of RDX before the irradiation along with (b) new bands observed in the spectrum in the high dose experiment at 5 K.

(a) Before Irradiation			
Wavenumber Observed (cm ⁻¹)	Wavenumber Literature (cm ⁻¹) ^[11]	Vibrational Assignments	Vibrational Modes
3079	3068	v ^{as} (CH ₂)	C-H asymm. stretch
2994	3004	v ^s (CH ₂)	C-H symm. stretch
1581	1576	v ^{as} (NO ₂)	NO ₂ asymm. stretch
1438	1435	β (CH ₂)	CH ₂ Bending in plane
1419	1424	γ (CH ₂)	CH ₂ Bending out of plane
1375	1391	γ (CH ₂)	CH ₂ Bending out of plane
1319	1322	v ^s (N-NO ₂)	N-N symm. stretch
1265	1275	v ^s (NO ₂)	NO ₂ symm. stretch
1217	1219	v (N-C-N)	Ring skeletal vibrations
1173	1160	v (N-C-N)	Ring skeletal vibrations
1081	1040	v ^{as} (Ring)	Ring asymm. vibrations
997	1020	v ^{as} (Ring)	Ring asymm. vibrations
933	947	v ^{as} (Ring)	Ring asymm. vibrations
908	882	v ^s (Ring)	Ring symm. vibrations
848	844	v (C-N-C)	Ring skeletal vibrations
786	790	v (C-N-C)	Ring skeletal vibrations
667	670	δ (Ring)	Ring deformation
(b) After Irradiation			
3513-3203		v(H ₂ O)	O-H stretch of H ₂ O

Table S2. Compilation of key experimental parameters of the infrared multiphoton decomposition studies of RDX.

Parameters	Low power	High power
Average power	10 W	24 W
Repetition rate	5 kHz	5 kHz
Pulse width	200 μ s	200 μ s
Beam radius	0.50 ± 0.05 cm	0.50 ± 0.05 cm
Irradiated area	0.8 ± 0.1 cm ²	0.8 ± 0.1 cm ²
Duration of exposure	240 min	240 min
Energy per pulse	2.0 mJ	4.8 mJ
Laser fluence	2.5 ± 0.2 mJ cm ⁻²	6.0 ± 0.6 mJ cm ⁻²
Total energy deposited	$1.8 \pm 0.2 \times 10^5$ J cm ⁻²	$4.3 \pm 0.4 \times 10^5$ J cm ⁻²
Penetration depth	3.6 ± 0.3 μ m	3.6 ± 0.3 μ m

Generation of VUV light

1. 10.49 eV –The third harmonics (355 nm) of a pulsed ND:YAG laser (Spectra Physics, PRO-250-30; 30 Hz) is exploited for generating 10.49 eV VUV light. The 355 nm light is focused on pulsed jet of Xenon (80 μ s, 30 Hz) which results in generation of 118 nm light (10.49 eV) via non-linear mixing. The 10.49 eV light is separated from 355 nm light by a LiF biconvex lens (ISP Optics) and directed 2 mm above the sample to ionize the subliming molecules.

2. 9.30 eV – The third harmonics (355 nm) of a pulsed ND:YAG laser (Spectra Physics, PRO-250-30; 30 Hz, 10 ns) is used to pump a dye laser (Sirah Cobra Stretch) having Coumarin 450 dye. The fundamental output of the dye laser (445 nm) undergoes frequency doubling to generate 222 nm (ω_1). Two photons of ω_1 is required to accesses the resonant transition of Xenon. The 532 nm light from a second ND:YAG laser (Spectra Physics, PRO-250-30; 30 Hz, 10 ns) is used to pump another dye laser (Sirah Cobra Stretch) containing LDS-698 dye to generate 672 nm (ω_2) light. The 222 nm and 672 nm lights are spatially and temporally overlapped on pulsed jet of Xenon (80 μ s, 30 Hz) which act as a non-linear medium. Difference frequency mixing of two photons of ω_1 and one photon of ω_2 in Xenon ($2\omega_1-\omega_2$) results in the generation of 133.3 nm (ω_{VUV} ; 9.30 eV) light. A LiF biconvex lens is used to separate the 133.3 nm light from residual 222 and 672 nm lights.

Table S3. Parameters for the Vacuum Ultraviolet Light (VUV) generation in the present study.

		ω_1				ω_2				
VUV Energy	Noble gas	YAG 1 (λ ; nm)	Dye	Dye laser (λ ; nm)	Wavelength after tripling (nm)	YAG 2 (λ ; nm)	Dye	Dye laser (λ ; nm)	Photons/pulse*	
10.49 eV	Xe	355	-	-	-	-	-	-	10^{14}	
9.30 eV	Xe	355	Coumarin 450	444	222	532 nm	LDS-698	672	10^{14}	

* 30Hz

Table S4. Coordinates of reactants and productsCoordinates of reactant, product and transition state (TS) of **Figure S6**.

Atom	X	Y	Z	Atom	X	Y	Z
RDX				TS (RDX-methylene nitramine)			
C	0.529913	0.032558	-1.205285	C	0.326445	1.639329	1.312196
N	0.336834	-1.034127	-0.216854	N	-1.45543	0.692343	0.886202
N	0.385173	1.336537	-0.583245	C	-1.58122	-0.53983	1.310875
C	-0.473355	-0.690347	0.966317	N	0.124951	-1.60165	0.885897
N	1.375432	-1.931909	-0.005291	C	1.254524	-1.0969	1.313853
N	-1.444722	0.304375	0.570509	N	1.327198	0.911987	0.885805
C	-0.909576	1.573085	0.06173	N	-2.03012	0.951493	-0.42061
N	-2.627613	-0.183872	-0.04439	N	0.190945	-2.23202	-0.41994
N	1.527782	1.830244	0.101891	N	1.839691	1.27982	-0.42189
O	-3.316821	0.635544	-0.621185	O	-1.63967	1.974857	-0.93885
O	-2.876531	-1.361106	0.110633	O	-2.86962	0.190131	-0.84819
O	1.363803	-2.509812	1.070391	O	-0.88893	-2.40421	-0.94142
O	2.164093	-2.096505	-0.916614	O	1.270964	-2.58151	-0.84233
O	2.586613	1.294205	-0.154919	O	2.524637	0.426939	-0.94242
O	1.352323	2.78112	0.838309	O	1.605943	2.389874	-0.8459
H	-0.235143	-0.033501	-1.977722	H	0.054765	2.55112	0.799113
H	1.506708	-0.079616	-1.657253	H	0.08267	1.547597	2.360587
H	0.143483	-0.262153	1.758855	H	-1.38347	-0.70439	2.360133
H	-0.971436	-1.571832	1.345219	H	-2.23545	-1.23036	0.797435
H	-1.622448	1.978847	-0.647871	H	1.295226	-0.84101	2.362658
H	-0.761105	2.280182	0.870932	H	2.180521	-1.321	0.803256

Methylene nitramine (H_2CNNO_2)			
C	1.7416	0.019042	0.129809
N	0.759161	-0.693176	-0.220598
N	-0.545822	0.019178	-0.027227
O	-0.566503	1.229645	-0.081628
O	-1.472072	-0.730117	0.133991
H	2.724813	-0.428399	0.035684
H	1.640803	1.035914	0.501331

Coordinates of reactant, products, intermediates and transition states (TS) of **Figure 3**.

Methylene nitramine (H_2CNNO_2)				I1 ((OH) CH_2NNO)		
C	1.7416	0.019042	0.129809	C	1.375618	0.068689
N	0.759161	-0.693176	-0.220598	N	0.294986	1.050396
N	-0.545822	0.019178	-0.027227	N	-0.540049	0.084800
O	-0.566503	1.229645	-0.081628	O	0.405960	-1.018515
O	-1.472072	-0.730117	0.133991	O	-1.718291	-0.044244
H	2.724813	-0.428399	0.035684	H	1.979094	0.071956
H	1.640803	1.035914	0.501331	H	1.981277	0.071606
I2 (c- H_2CNNO_2)				I3 (H_2CNNOO)		
C	1.713192	0.292332	-0.149189	C	2.17045	0.17784
N	0.881402	-0.643752	0.028766	N	1.06529	-0.46894
N	-0.343721	-0.311144	0.587977	N	0.00000	0.37745
O	-0.929981	0.891716	0.030062	O	-2.18123	0.21966
O	-1.348428	-0.445534	-0.399076	O	-1.04121	-0.38154
H	2.699964	0.021668	-0.50429	H	3.08702	-0.39663
H	1.484392	1.33916	0.034336	H	2.21272	1.26501

Diazomethane (H_2CNN)				TS (methylene nitramine - I2)			
C	0.00000	0.00000	-1.13686	C	1.75263	0.205857	-0.117856
N	0.00000	0.00000	0.15560	N	0.844722	-0.668162	0.059895
H	0.00000	0.95023	-1.64050	N	-0.402474	-0.201724	0.415269
H	0.00000	-0.95023	-1.64050	O	-0.842302	1.099674	-0.020094
N	0.00000	0.00000	1.28757	O	-1.39907	-0.63237	-0.257185
				H	2.759639	-0.158479	-0.278109
				H	1.559825	1.27411	-0.122671
TS (I2 - I1)				TS (I2 - diazomethane + oxygen)			
C	1.890868	0.447411	-0.11838	C	1.679457	0.559221	-0.107527
N	1.029786	-0.46797	0.011965	N	0.999928	-0.492175	0.098731
N	-0.14624	-0.36992	0.563368	N	-0.13073	-0.880325	0.344449
O	-1.68245	0.704688	0.022812	O	-1.362826	0.689414	0.385149
O	-1.07486	-0.51504	-0.39044	O	-1.146482	-0.156136	-0.648091
H	2.872182	0.180487	-0.48842	H	2.712913	0.465879	-0.405274
H	1.656299	1.483074	0.112376	H	1.200427	1.520072	0.051707
TS (I3 - diazomethane + oxygen)				TS (methylene nitramine-I1)			
C	2.302563	-0.13684	0.1747	C	1.520730	0.095891	0.112629
N	1.081317	-0.02918	-0.1868	N	0.493041	0.932926	-0.122590
N	0.079094	0.634515	-0.19645	N	-0.496148	0.048048	-0.014712
O	-2.28247	0.061252	0.171362	O	0.025480	-1.160137	-0.119254
O	-1.16243	-0.44011	-0.05022	O	-1.669518	0.258907	0.085796
H	2.898038	-0.94061	-0.23241	H	1.638108	-0.422607	1.058947
H	2.722914	0.555172	0.897822	H	2.411570	0.190284	-0.505949
TS (I1 - formaldehyde + dinitrogen monoxide)							
C	1.372097	-0.179151	0.079239				
N	0.035742	-1.076000	-0.107789				
N	-0.732519	-0.178022	0.015891				
O	0.887142	1.041552	-0.066856				
O	-1.776919	0.321979	0.033386				
H	2.119834	-0.524156	-0.651756				

H	1.643237	-0.531035	1.087368	
---	----------	-----------	----------	--

Coordinates of reactants, products, intermediates and transition states (TS) of **Figure 4**.

Atom	X	Y	Z	Atom	X	Y	Z
Formaldehyde (H ₂ CO)				Carbon monoxide (CO)			
C	0.000000	0.000000	-0.525972	C	0.000000	0.000000	-0.643517
O	0.000000	0.000000	0.673063	O	0.000000	0.000000	0.482638
H	0.000000	0.937504	-1.114339				
H	0.000000	-0.937504	-1.114339				
Ketene (H ₂ CCO)				Methanol (CH ₃ OH)			
O	0.000000	0.000000	1.262345	H	-0.86439	-1.06218	0.00000
C	0.000000	0.000000	-1.205880	H	-0.43840	1.08011	0.88898
H	0.000000	0.937571	-1.737695	C	0.04662	0.66339	0.00000
H	0.000000	-0.937571	-1.737695	O	0.04662	-0.75719	0.00000
C	0.000000	0.000000	0.101985	H	-0.43840	1.08011	-0.88898
				H	1.08847	0.97913	0.00000
TS (formaldehyde – methanol + carbon monoxide)				TS (methanol + carbon monoxide – ketene + water)			
C	-0.970214	-0.069050	-0.000008	C	0.377701	-0.460618	-0.019997
O	-2.111633	0.070975	0.000004	O	2.292498	0.282690	0.116425
H	0.003050	-0.874563	-0.000012	H	0.608356	0.606724	0.100921
H	0.028952	0.903301	-0.000002	H	0.558982	-0.918046	-0.980111
C	1.420157	0.563930	0.000000	C	-1.310328	-0.357658	-0.005932
O	1.345567	-0.717207	0.000003	O	-2.125437	0.440267	0.009102
H	1.698436	1.085917	-0.924591	H	0.593559	-1.093739	0.825082
H	1.698432	1.085921	0.924589	H	2.498384	0.531057	-0.794536

2-hydroxyacetaldehyde				TS (Formaldehyde - 2-hydroxyacetaldehyde)			
C	0.521362	0.528597	0.081215	C	-0.917940	0.663596	-0.012629
C	-0.728870	-0.337931	0.141166	O	-1.172620	-0.623683	-0.221690
O	-1.832208	0.048103	-0.141486	H	-0.687246	1.284105	-0.879498
H	0.579846	1.079838	1.026158	H	-1.450305	1.150025	0.807803
H	0.408565	1.265939	-0.723198	H	-0.013912	-1.216377	0.331449
O	1.709874	-0.237011	-0.011570	C	0.628814	-0.107570	0.405570
H	-0.532589	-1.378062	0.487746	O	1.606513	0.059028	-0.289291
H	1.767890	-0.600457	-0.900543	H	0.415080	-0.036667	1.470444
TS (2-hydroxyacetaldehyde- water + ketene)							
C	-0.340343	0.799288	-0.004684				
C	0.711030	-0.249076	-0.014690				
O	1.909119	-0.172443	0.023988				
H	-0.593171	1.330541	-0.917001				
H	-0.613820	1.299677	0.922694				
O	-1.660044	-0.378314	-0.093790				
H	-0.887509	-1.090069	-0.094529				
H	-2.122221	-0.435362	0.763492				

Table S6. Calculated harmonic frequencies and intensities of the reactants, products and intermediates.

Frequencies and intensities of reactants, products and transition states of Figure S5.

		RDX	TS (RDX-methylene nitramine)	
Normal modes	Frequency(cm ⁻¹)	IR Inten	Frequency(cm ⁻¹)	IR Inten
v1	29.76	8.734	-406.58	0.6562
v2	47.83	2.0036	27.98	0.7813
v3	63.46	2.3436	34.24	2.3993
v4	78.46	0.2617	37.9	1.1724
v5	87.22	1.5664	73.48	17.0297
v6	118.29	0.9456	76.13	17.7329
v7	205.22	3.1277	84.06	1.564
v8	230.78	5.5047	129.69	51.265
v9	249.7	1.7434	131.49	50.4967
v10	338.05	1.437	177.82	3.6939
v11	360.36	3.9289	186.18	59.4232
v12	392.71	2.5485	187.44	64.4377
v13	415.02	1.4919	383.46	28.1478
v14	428.22	5.8062	386.1	30.9127
v15	453.67	12.831	407.75	11.7648
v16	593.94	18.8045	411.22	68.7948
v17	607.48	21.0429	411.54	70.4194
v18	613.42	1.7884	462.51	23.5445
v19	645.42	4.5259	586.15	34.8332
v20	684.05	0.0335	586.51	34.7636
v21	763.35	1.1631	599.08	1.3953
v22	774.69	4.234	657.46	54.9673
v23	779.65	44.8987	658.74	55.0264
v24	795.32	9.8922	662.26	3.9452
v25	847.78	2.4809	760.75	17.9562

v26	868.66	26.348	767.23	13.758
v27	893.28	9.3538	767.95	13.7533
v28	921.77	364.2882	849.76	127.3277
v29	941.55	4.2217	850.18	127.8275
v30	979.31	33.6716	878.51	125.1796
v31	1017.07	181.4937	945.58	2.5032
v32	1136.66	59.2749	948.17	2.7747
v33	1151.39	91.2138	953.77	4.3562
v34	1185.57	23.7189	1079.9	63.8174
v35	1228.5	25.8059	1128.03	37.6555
v36	1240.36	29.2388	1130.82	37.9393
v37	1283.05	212.7402	1192.98	15.9506
v38	1295.97	258.9685	1206.29	4.5892
v39	1301.26	361.4362	1206.7	4.2409
v40	1315.46	47.5426	1298.3	278.332
v41	1338.24	55.2666	1298.53	276.7939
v42	1354.61	22.5569	1322.75	365.5599
v43	1379.23	1.1924	1357.83	30.9773
v44	1408.32	29.1051	1384.8	52.5449
v45	1417.68	43.9747	1386.35	53.8507
v46	1493.21	51.5968	1517.28	10.2447
v47	1499.85	33.3449	1532.63	29.7198
v48	1513.06	13.352	1534.96	30.2782
v49	1622.19	197.2842	1639.17	5.6418
v50	1645.57	210.3287	1665.11	385.2494
v51	1646.02	479.0827	1666.01	384.0746
v52	3051.36	8.5695	3144.92	7.9936
v53	3076.99	10.3326	3145.36	11.5921
v54	3117.05	0.2252	3146.85	10.157
v55	3164.46	7.5657	3245.25	8.1385
v56	3186.16	10.2461	3245.89	6.1636

v57	3189.37	3.2475	3247.6	3.5125
Methylene nitramine (H_2CNNO_2)				
Normal modes	Frequency(cm^{-1})		IR Inten	
v1	20.1		9.3367	
v2	386.01		5.5683	
v3	515.75		6.1796	
v4	525.15		9.0964	
v5	699.72		2.0759	
v6	844.02		81.5395	
v7	884.97		10.0959	
v8	1097.05		21.1081	
v9	1181.96		2.2406	
v10	1338.95		168.9888	
v11	1433.33		34.2904	
v12	1678.24		248.9754	
v13	1705.4		104.5688	
v14	3091.05		6.3999	
v15	3198.35		0.2199	

Frequencies and intensities of reactants, products and transition states of Figure 3.

Methylene nitramine (H_2CNNO_2)		$\text{I1} ((\text{OH})\text{CH}_2\text{NNO})$		
Normal modes	Frequency(cm^{-1})	IR Inten	Frequency(cm^{-1})	IR Inten
v1	20.1	9.3367	310.79	4.5386
v2	386.01	5.5683	487.1	20.1219
v3	515.75	6.1796	700.09	10.2239
v4	525.15	9.0964	769.52	86.0317
v5	699.72	2.0759	904.95	60.6674
v6	844.02	81.5395	989.25	61.8714
v7	884.97	10.0959	1052.49	19.7008
v8	1097.05	21.1081	1068.47	4.0021
v9	1181.96	2.2406	1101.98	2.2829
v10	1338.95	168.9888	1215.33	33.5359
v11	1433.33	34.2904	1361.18	33.7886
v12	1678.24	248.9754	1504.63	4.8661
v13	1705.4	104.5688	1779.34	554.2063
v14	3091.05	6.3999	3066.77	19.4238
v15	3198.35	0.2199	3128.44	8.6794

$\text{I2} (\text{e-H}_2\text{CNNO}_2)$		$\text{I3} (\text{H}_2\text{CNNOO})$		
Normal modes	Frequency(cm^{-1})	IR Inten	Frequency(cm^{-1})	IR Inten
v1	149.12	7.4827	138.8	4.9794
v2	317.58	8.2623	285.71	1.0381
v3	469.91	3.0519	308.32	7.863
v4	588.16	5.0157	583.65	2.9292
v5	725.77	30.482	618.36	14.615
v6	741.5	7.3719	726.2	0.2815
v7	893.55	3.9016	1037.02	1.9899
v8	898.96	22.7634	1053.7	23.9691
v9	1057.93	23.0443	1115.17	114.7861
v10	1138.02	53.8093	1197.43	137.4781
v11	1204.17	2.7974	1291.44	7.7905
v12	1470.21	13.938	1450.46	31.7821
v13	1699.67	5.6904	1642.76	19.3713
v14	3091.93	7.0252	3087.75	6.9709
v15	3202.59	3.7818	3218.46	2.0193

		Diazomethane (H₂CNN)		TS (methylene nitramine - I2)	
Normal modes	Frequency(cm ⁻¹)	IR Inten	Frequency(cm ⁻¹)	IR Inten	
v1	430.32	430.32	-1252.68	341.1511	
v2	434.91	434.91	128.79	7.9624	
v3	583.88	583.88	305.57	9.1823	
v4	1119.63	1119.63	437.75	3.0503	
v5	1209.91	1209.91	583.89	3.0004	
v6	1441.29	1441.29	702.71	6.4609	
v7	2202.42	2202.42	801.21	2.5899	
v8	3186.49	3186.49	883.55	26.1951	
v9	3308.86	3308.86	1045.29	23.8224	
v10			1164.85	3.8443	
v11			1242.04	13.9977	
v12			1457.44	16.7864	
v13			1654.74	6.3912	
v14			3102.63	3.5167	
v15			3212.46	1.2535	
TS (I2 - I1)			TS (I2 - diazomethane + oxygen)		
Normal modes	Frequency(cm ⁻¹)	IR Inten	Frequency(cm ⁻¹)	IR Inten	
v1	-453.33	7.1936	-578.97	15.9752	
v2	139.52	5.4624	178.51	3.2045	
v3	211.61	34.4436	185.43	27.4789	
v4	408.46	11.3407	321.45	19.1967	
v5	554.65	39.791	472.12	12.695	
v6	801.04	12.7553	622.82	4.9487	
v7	848.32	38.4743	734.59	4.7592	
v8	1044.33	45.4566	942.82	38.0523	
v9	1050.82	21.0767	1097.85	39.7914	
v10	1136.01	119.8612	1136.18	43.3482	
v11	1191.02	12.5156	1203.39	49.6261	
v12	1493.4	12.116	1486.11	4.6631	
v13	1708.56	23.3262	1743.9	13.959	
v14	3096.88	3.9775	3112.22	2.902	
v15	3217.23	1.037	3247.73	0.9613	

		TS (I3 - diazomethane + oxygen)		TS (methylene nitramine-I1)	
Normal modes	Frequency(cm ⁻¹)	IR Inten	Frequency(cm ⁻¹)	IR Inten	
v1	-509.89	4.8031	-759.31	22.2061	
v2	126.48	3.6744	292.44	8.6087	
v3	193.58	78.5115	584.78	4.2635	
v4	246.36	1.8172	766.62	15.3847	
v5	370.26	40.9693	786.13	18.1457	
v6	563.61	136.2792	809.82	44.8589	
v7	720.25	1.632	1000.52	10.704	
v8	842.53	47.3784	1071.43	55.1828	
v9	1128.07	33.4457	1144.21	39.8056	
v10	1199.45	8.9703	1231.78	92.4092	
v11	1314.69	459.2275	1292.07	80.7448	
v12	1507.73	2.7067	1536.8	35.5605	
v13	1726.18	24.186	1662.03	407.6588	
v14	3096.01	2.4265	3078.35	11.2167	
v15	3224.75	1.5202	3170.52	4.9067	

TS (I1 - formaldehyde + dinitrogen monoxide)		
Normal modes	Frequency(cm ⁻¹)	IR Inten
v1	-1092.24	184.1696
v2	201.93	6.066
v3	248.54	33.9012
v4	502.37	43.2283
v5	635.36	225.3027
v6	732.76	18.6331
v7	995.68	25.4822
v8	1114.84	28.8471
v9	1153.63	8.2213
v10	1254.14	78.2679
v11	1361.15	63.3187
v12	1515.78	11.3099
v13	2035.55	520.79
v14	2922.26	79.688
v15	2964.23	62.335

Frequencies and intensities of reactants, products and transition states of Figure 4.

		Formaldehyde (H ₂ CO)		Carbon monoxide (CO)	
Normal modes		Frequency(cm ⁻¹)	IR Inten	Frequency(cm ⁻¹)	IR Inten
v1		1202.72	3.2324	2211.46	74.7425
v2		1268.59	12.8091		
v3		1536.28	9.8978		
v4		1823.93	106.9135		
v5		2876.66	68.9749		
v6		2930.91	144.456		
		Ketene (H ₂ CCO)		Methanol (CH ₃ OH)	
v1		442.73	2.5442	300.4	110.6229
v2		552.4	61.6686	1045.3	118.8796
v3		591.79	66.3665	1082.56	1.0568
v4		991.34	5.8031	1170.03	0.5851
v5		1171.08	5.181	1375.1	26.6663
v6		1412.39	17.7177	1481.51	3.9015
v7		2221.3	625.2583	1494.78	2.0055
v8		3181.36	27.0814	1512	3.8831
v9		3274.2	8.5356	2986.07	63.2785
v10				3027.87	67.9868
v11				3102.58	30.0351
v12				3829.25	25.2573
TS (formaldehyde – methanol + carbon monoxide)			TS (methanol + carbon monoxide – ketene + water)		
v1	-1594.38	457.4394	-828.48	7.48	
v2	126.83	10.8002	107.84	25.2031	
v3	361.38	15.9778	179.89	26.5856	
v4	511.23	15.7115	305.44	52.0923	
v5	532.88	4.7113	356.72	18.5713	
v6	679.52	105.3251	373.8	7.079	
v7	956.52	4.9209	496.74	7.0382	
v8	1084.3	192.7653	776.34	31.6147	
v9	1219.92	5.1757	826.01	308.2623	
v10	1248.32	2.6782	1076.62	0.9749	
v11	1320.87	205.9157	1148.16	8.2511	
v12	1428.7	83.8864	1341.56	4.1778	
v13	1464.21	25.589	1385.93	18.2266	

v14	1579.05	36.6014	2077.15	646.4704
v15	1887.02	57.3604	2979.36	90.9968
v16	2080.8	309.253	3206.79	14.0392
v17	2955.39	45.7807	3270.93	3.5896
v18	3021.45	70.5907	3771.48	20.4041

2-hydroxyacetaldehyde		TS (Formaldehyde - 2-hydroxyacetaldehyde)
v1	87.7	-1811.9140
v2	327.7	263.7248
v3	343.2	322.5682
v4	524.4	469.4562
v5	722.6	666.0692
v6	1031.5	840.7301
v7	1066.4	875.6615
v8	1081.6	1028.2352
v9	1207.8	1080.2455
v10	1336.4	1139.5213
v11	1393.2	1195.7924
v12	1396.2	1299.1323
v14	1467.1	1530.9297
v15	1821.2	1641.9978
v16	2865.2	1892.1636
v17	3013.2	3028.3154
v18	3062.5	3126.5331
v19	3831.0	3144.3180

TS (2-hydroxyacetaldehyde- water + ketene)

v1	-922.0549
v2	220.9385
v3	311.1545
v4	432.4269
v5	617.7561
v6	667.8070
v7	703.8876
v8	812.9731
v9	883.2888
v10	1038.3189
v11	1105.0833
v12	1398.0224

v14	1473.1369
v15	1806.3505
v16	2303.4941
v17	3079.0966
v18	3194.0045
v19	3641.5629

References:

- [1] a) B. M. Jones, R. I. Kaiser, *J. Phys. Chem. Lett.* **2013**, *4*, 1965-1971; b) R. I. Kaiser, S. Maity, B. M. Jones, *Phys. Chem. Chem. Phys.* **2014**, *16*, 3399-3424; c) C. J. Bennett, S. J. Brotton, B. M. Jones, A. K. Misra, S. K. Sharma, R. I. Kaiser, *Anal. Chem.* **2013**, *85*, 5659-5665.
- [2] R. A. Isbell, M. Q. Brewster, *Propellants, Explos., Pyrotech.* **1998**, *23*, 218-224.
- [3] A. D. Becke, *J. Chem. Phys.* **1992**, *96*, 2155-2160.
- [4] a) C. Hampel, K. A. Peterson, H.-J. Werner, *Chem. Phys. Lett.* **1992**, *190*, 1-12; b) P. J. Knowles, C. Hampel, H. J. Werner, *J. Chem. Phys.* **1993**, *99*, 5219-5227.
- [5] K. A. Peterson, D. E. Woon, T. H. D. Jr., *J. Chem. Phys.* **1994**, *100*, 7410-7415.
- [6] M. J. T. Frisch, G. W.; Schlegel, H. B.; Scuseria, G. E.; Robb, M. A.; Cheeseman, J. R.; Scalmani, G.; Barone, V.; Petersson, G. A.; Nakatsuji, H.; Li, X.; Caricato, M.; Marenich, A. V.; Bloino, J.; Janesko, B. G.; Gomperts, R.; Mennucci, B.; Hratchian, H. P.; Ortiz, J. V.; Izmaylov, A. F.; Sonnenberg, J. L.; Williams-Young, D.; Ding, F.; Lipparini, F.; Egidi, F.; Goings, J.; Peng, B.; Petrone, A.; Henderson, T.; Ranasinghe, D.; Zakrzewski, V. G.; Gao, J.; Rega, N.; Zheng, G.; Liang, W.; Hada, M.; Ehara, M.; Toyota, K.; Fukuda, R.; Hasegawa, J.; Ishida, M.; Nakajima, T.; Honda, Y.; Kitao, O.; Nakai, H.; Vreven, T.; Throssell, K.; Montgomery, J. A., Jr.; Peralta, J. E.; Ogliaro, F.; Bearpark, M. J.; Heyd, J. J.; Brothers, E. N.; Kudin, K. N.; Staroverov, V. N.; Keith, T. A.; Kobayashi, R.; Normand, J.; Raghavachari, K.; Rendell, A. P.; Burant, J. C.; Iyengar, S. S.; Tomasi, J.; Cossi, M.; Millam, J. M.; Klene, M.; Adamo, C.; Cammi, R.; Ochterski, J. W.; Martin, R. L.; Morokuma, K.; Farkas, O.; Foresman, J. B.; Fox, D. J., *Gaussian 16, Revision C.01, Gaussian, Inc.: Wallingford, CT, 2016*.
- [7] M. S. a. L. SZYMAŃCZYK, *Cent. Eur. J. Energ. Mater.* **2014**, *11*, 129-142.
- [8] C. J. Bennett, S. H. Chen, B. J. Sun, A. H. H. Chang, R. I. Kaiser, *Astrophys. J.* **2007**, *660*, 1588-1608.
- [9] P. A. S. Gerakines, W. A.; Greenberg, J. M.; van Dishoeck, E. F., *Astron. Astrophys.* **1995**, *296*, 810-818.
- [10] D. Fulvio, B. Sivaraman, G. A. Baratta, M. E. Palumbo, N. J. Mason, *Spectrochim. Acta, Part A* **2009**, *72*, 1007-1013.
- [11] K. S. Z. Iqbal, S. Bulusu, J. R. Autera, *National Technical Information Service, U.S. Department of Commerce, Springfield VA*.